Renewable Energy, Environment, and Power Quality Journal (REE&PQJ)
ISSN:3020-531X
Volume 26, July 2026

Enhanced Power Control for Voltage Support Strategy and Virtual Inertia Emulation for Distributed Battery Energy Storage System

Ahmed Alharbi [1], Fahd Hariri[1], and Yusuf Alturki[1,2]

[1] Department of Electrical and Computer Engineering, Faculty of Engineering, King Abdulaziz University, 6 Jeddah 4 21589, Saudi Arabia; yaturki@kau.edu.sa; smalgamdi1@kau.edu.sa; mrawa@kau.edu.sa
[2] Research and Innovation Center, King Abdulaziz University, Jeddah 21589, Saudi Arabia
Ahmad.e.s1991@gmail.com

Abstract. In active distribution systems, the battery energy storage system (BESS) can support grid stability through coordinated active and reactive power control mechanisms. Therefore, this paper proposes a coordinated control scheme for BESS to voltage and frequency regulations under dynamic operating conditions. For inertia emulation control, a coupling mechanism between the rate of change of frequency (RoCoF) combined with voltage magnitude and the required active power of grid is studied. Meanwhile, a coupling mechanism between the rate of change of voltage (RoCoV) and frequency magnitude is employed to regulate reactive power injection for effective voltage support. Based on the grid-voltage modulated direct power control (GVMDPC), the inner control loop is designed to accurately track both active and reactive power references, ensuring better dynamic performance of the grid-connected battery energy storage. Intensive simulation studies that have been conducted on a wind-BESS system are executed using MATLAB/ Simulink platform along with the validation of the proposed scheme. Finally, simulations are performed to assess the capability of the proposed control scheme to improve the dynamic response of grid frequency and voltage compared with the conventional method.

Keywords. Voltage support, virtual inertia emulation, coordinated control, Renewable energies, and Battery Energy storage systems.

1. Introduction

Renewable Energy (RE) sources are increasingly integrated into power grids around the world. They provide clean and sustainable energy and can be more economical over a long period of time. However, their integration also introduces several challenges. Most renewable energy systems are inverter-based and provide little or no inertia to the grid. As a result, the system becomes more sensitive to disturbances, which can weaken grid stability. Added to that the low inertia in modern grids due to the lack of rotational momentum typically provided by synchronous generators (SGs) causes power shortages and, in some cases, blackouts [1], [2]. While blackouts can be temporarily managed in islanding mode until the issues are resolved, a safer and more effective solution is to add a Battery Energy Storage System (BESS). The BESS boosts overall reliability, provides backup power under heavy loading, and can emulate virtual inertia in the grid [3]. Furthermore, communication between SGs, renewable generators (RGs), and BESS can be established using traditional voltage and frequency control methods, such as automatic voltage regulators (AVRs) in synchronous generation and droop control. However, these conventional methods do not provide optimized responses in dynamic and complex system conditions such as active distribution systems [4].

Recently, the cascaded feedback loops voltage and frequency controllers have been adopted to control the BESS integrated with the grid-side inverter [5], [6], [7]. To manage the BESS discharging or charging current, several studies are commonly utilized an inner current control loop [8], [9]. For the BESS grid-side inverter, an outer voltage control loop is typically implemented to maintain the DC-bus voltage aligned with the generating the d-axis current reference. Meanwhile, the inner current control loop regulates the d-axis current to control the active power flow, while the q-axis current is used to regulate the reactive power flow [10], [11], [12]. Another approach is Direct Power Control (DPC), which has been implemented in [13], [14], [15]. This method provides faster dynamic response and smoother synchronization, enabling rapid regulation of active and reactive power. Furthermore, recent studies have improved this approach by introducing Grid-Voltage Modulated Direct Power Control (GVM-DPC). This technique offers a faster instantaneous response to changes in active and reactive power compared with conventional controllers [16].

To track voltage and frequency variations, the Phase-Locked Loop (APLL) is widely applied, as discussed in [17], [18], [19]. As shown in Fig.1, a APLL typically consists of three main components: a phase detector, a loop filter, and a voltage-controlled oscillator.

Through this structure, frequency variations can be identified from the phase shift angle $\boldsymbol{\theta}$. Recently, several studies have combined the Amplitude-Locked Loop (ALL) with the PLL to enhance disturbance detection [14]. This combined structure, known as the Amplitude Phase-Locked Loop (APLL), enables the detection of voltage deviation $(\boldsymbol{\Delta V})$, frequency deviation $(\boldsymbol{\Delta f})$, and their transient rates $(\boldsymbol{dV/dt})$and $(\boldsymbol{df/dt})$ [15]. These signals can then be used to mimic the rate of change of frequency (RoCoF) and rate of change of voltage (RoCoV). In this approach, the BESS compensates for power imbalances by injecting or absorbing power, thereby improving system stability and mitigating the effects of low inertia in the weak grid.

To achieve flexible power regulation, some researchers have made significant efforts on the coordinated and frequency control as in [20], [21], [22], [23]. In [16], the inertial and voltage support capability of BESS are employed the $(\boldsymbol{dV/dt})$ and $(\boldsymbol{df/dt})$ to regulate the active and reactive power, respectively. In [17], the authors utilize the (dV/dt)signal for voltage support; however, the inertia regulation capability is not considered. In [18], the virtual battery algorithm is used for voltage and frequency regulations, which decouple the inertia and droop control parts. However, it lacks dynamics damping, leading to high level frequency or voltage oscillations. In [19], a double-loop active and reactive control is proposed for a BESS grid-side inverter. This scheme relied on frequency deviation (Δf) to regulate voltage control, which makes the voltage sensitivity significantly affected grid voltages. However, the control loops are not fully considered the variation in voltage, and not competent for BESS charging and discharging.

In this paper, a novel inertia–voltage control model is proposed for the grid-side inverter of the Battery Energy Storage System (BESS). The rate of change of voltage $(dV/dt)$and frequency deviation (Δf) are employed as control inputs for active power regulation. In addition, the rate of change of voltage $(dV/dt)$and voltage deviation (ΔV) are utilized as control inputs to regulate reactive power through the grid-connected inverter, thereby enhancing voltage support and system stability. The simulations are conducted by comparing the control model presented in [24]with the proposed model to demonstrate the superiority and effectiveness of the proposed control strategy.

2. Proposed Model Control for Inertia and Voltage Regulation

2.1 Extracting voltage and frequency variations-based APLL

For voltage and frequency magnitude estimation, an advanced APLL system is adopted as shown in Fig.1 [16]. This system utilizes the three-phase voltage signals measured at the point of common coupling (PCC) to determine the control input parameters, including the rate of change of voltage (dV/dt), frequency deviation (Δf), and voltage deviation (ΔV). To constitute the control implementation, the Park transformation [20] is applied to convert the grid signals into the dqreference frame, which serves as the input to the control system. the APLL dynamic equations can be expressed as follows [19]:

$$U_{apll} = \frac{1}{k_a}\int v_d \, dt \tag{1}$$

$$\frac{dU_{apll}}{dt} = \frac{1}{k_a}(v_d - U_{apll}) \tag{2}$$

$$\theta_{apll} = \frac{1}{k_a}\int (\omega_{apll} + K_{pll}\frac{d\omega_{apll}}{dt}) \, dt \tag{3}$$

$$\frac{d\theta_{apll}}{dt} = \frac{1}{k_a}(\omega_{apll} + K_{pll}\frac{d\omega_{apll}}{dt}) \tag{4}$$

$$\omega_{apll} = \frac{1}{k_p}\int v_q \, dt \tag{5}$$

$$\frac{d\omega_{apll}}{dt} = \frac{1}{k_p}v_q \tag{6}$$

where $v_d$and $v_q$represent the d-axis and q-axis voltages at the Point of Common Coupling (PCC). U_{apll} and $\frac{dU_{apll}}{dt}$denote the estimated voltage amplitude and its rate of change, respectively. Furthermore, θ_{apll} and ω_{apll}represent the estimated phase angle and angular frequency, while $\frac{d\theta_{apll}}{dt}$and $\frac{d\omega_{apll}}{dt}$denote their corresponding dynamic variations.

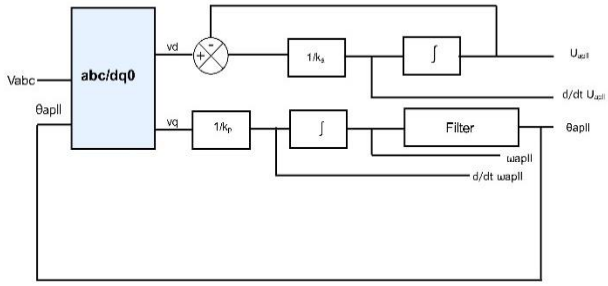

Fig.1 Block diagram of APLL to estimate the voltage and frequency variations.

2.2 Control Structure

In this paper, a model-based BESS control framework is developed to validate the voltage and frequency regulation in the low inertial weak grids. First, the proposed inertia control are designed based on $(dV/dt)$and (Δf) to control the active power, while (df/dt) and voltage deviation (ΔV) are employed to regulate the reactive power. For inertia emulating control APLL as depicted in Fig.2, the inverter active power reference mainly controls frequency stability, which can be mathematically expressed as follows,

$$P_e^* = P_{\Delta f}^* + P_{dv}^* \tag{7}$$

where:

$P_{\Delta f}^*$ and P_{dv}^* refer to the active power references yielded from frequency support control (Δf) and dynamic voltage responses control (dV/dt).

$$\cdot\begin{cases} P_{\Delta f}^* = K_{\Delta f}(\omega_g^* - \omega_{apll}) \\ P_{dv}^* = \frac{K_{dv}}{T_{dv}s+1} \cdot \frac{dU_{apll}}{dt} \end{cases} \tag{8}$$

The parameters $K_{\Delta f}$and K_{dv}represent the gains associated with active power control, while T_{df}denotes the time constant of the low-pass filter (LPF), which is used to suppress harmonics and measurement noise. The signals $\omega_{apll}$and $\frac{dU_{apll}}{dt}$correspond to the grid frequency and the rate of change of voltage, respectively, both estimated by the APLL. The term ω_g^* represents the nominal grid frequency.

For dynamic voltage regulation control as shown in Fig.2, the inverter reactive power reference mainly controls voltage stability, which can be formulated as follows,

$$Q_e^* = Q_{\Delta v}^* + Q_{df}^* \tag{9}$$

where:

$Q_{\Delta v}^*$and Q_{df}^* refer to the reactive power references generated from frequency support control (Δv) and inertia emulation control (df/dt).

$$
\begin{cases} Q_{\Delta v}^* = K_{\Delta V}\left(U_m^* - U_{apll}\right) \\ Q_{df}^* = \frac{K_{df}}{T_{df}s+1} \cdot \frac{d\omega_{apll}}{dt} \end{cases} \quad (10)
$$

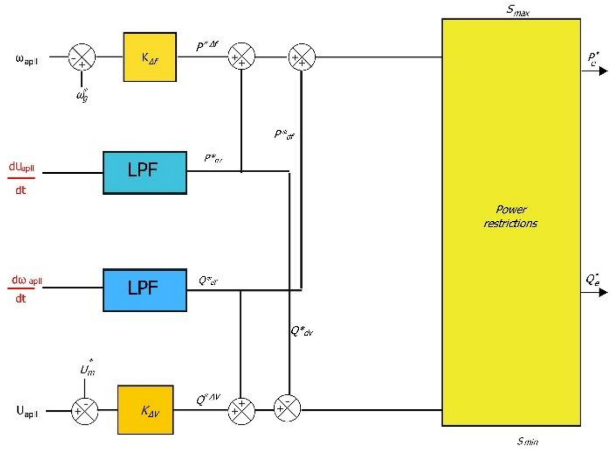

Fig.2 Virtual inertia emulation control and voltage regulation based on the APLL.

2.3 *Proposed GVM-DPC-Based Fast Power Control for BESS*

The grid-side converter dynamics are represented in the stationary $\alpha\beta$reference frame using the Clarke transformation. The relationship between the converter output voltage and the grid variables is given by:

$$
u_\alpha = Ri_\alpha + L\frac{di_\alpha}{dt} + v_\alpha \quad (11)
$$

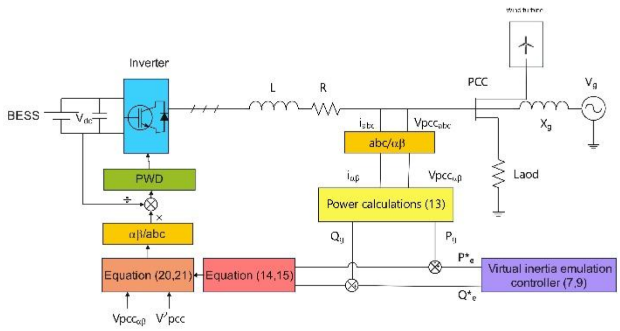

Fig.3 Control diagram of BESS-based GVM-DPC for a Weak grid structure for simulation study.

$$
u_\beta = Ri_\beta + L\frac{di_\beta}{dt} + v_\beta \quad (12)
$$

where $u_\alpha, u_\beta$are the converter output voltages, $R$and Lrepresent the filter resistance and inductance, respectively, $v_\alpha, v_\beta$are the grid voltages, and $i_\alpha, i_\beta$are the grid currents.

The instantaneous active and reactive powers in the $\alpha\beta$frame are expressed as:

$$
\begin{bmatrix} P \\ Q \end{bmatrix} = \frac{3}{2}\begin{bmatrix} v_\alpha & v_\beta \\ v_\beta & -v_\alpha \end{bmatrix}\begin{bmatrix} i_\alpha \\ i_\beta \end{bmatrix} \quad (13)
$$

where $P$and Qdenote the instantaneous active and reactive power, respectively.

By differentiating (13) and substituting (11) and (2), the dynamics of active and reactive power can be derived as:

$$
\frac{dP}{dt} = -\frac{R}{L}P - \omega Q + \frac{3}{2L}u_P \quad (14)
$$

$$
\frac{dQ}{dt} = -\frac{R}{L}Q + \omega P + \frac{3}{2L}u_Q \quad (15)
$$

The voltage-modulated control inputs used in the Grid-Voltage-Modulated Direct Power Control (GVM-DPC) are defined as:

$$
u_P = u_\alpha v_\alpha + u_\beta v_\beta - V_g^2 \quad (16)
$$

$$
u_Q = u_\alpha v_\beta - u_\beta v_\alpha \quad (17)
$$

where $u_P$and $u_Q$are auxiliary control inputs, and $V_g = \sqrt{v_\alpha^2 + v_\beta^2}$is the magnitude of the grid voltage.

Using the converter output voltages and currents, the power exchanged between the BESS and the grid is given by:

$$
P_g = \frac{3}{2}\left(v_\alpha i_\alpha + v_\beta i_\beta\right) \quad (18)
$$

$$
Q_g = \frac{3}{2}\left(v_\beta i_\alpha - v_\alpha i_\beta\right) \quad (19)
$$

Finally, the converter voltage references used for PWM generation can be obtained by inverting (16) and (17):

$$
u_\alpha = \frac{u_P v_\alpha - u_Q v_\beta}{V_g^2} \quad (20)
$$

$$
u_\beta = \frac{u_P v_\beta + u_Q v_\alpha}{V_g^2} \quad (21)
$$

The power exchange of the BESS is limited by its State of Charge (SOC), which determines its ability to supply or absorb energy based on its maximum capacity. Its impact on grid stability also depends on load characteristics, where active power support helps regulate frequency, while high reactive power demand may cause voltage instability or collapse. Additionally, during charging, the BESS can act as a load, potentially leading to voltage and frequency fluctuations. To prevent such critical conditions and ensure the protection of sensitive equipment, voltage deviations are constrained using the CBEMA curves as shown in Fig.4 which define acceptable voltage magnitude limits based on disturbance duration, thereby maintaining safe and reliable system operation.

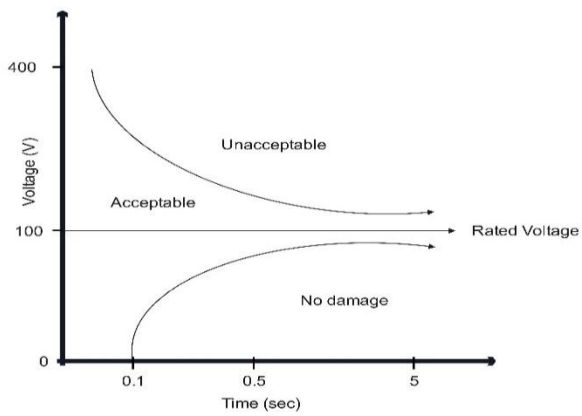

Fig.4 CBEMA curve.

3. Case study: Application of the proposed control strategy

3.1 System description

In this study, a medium-voltage distribution system is implemented to demonstrate the effectiveness of a distributed BESS in providing enhanced grid support services. As shown in Fig. 5, the network consists of a swing bus (Bus 1 at 10 kV), two transmission lines, and Bus 3, which serves as the point of common coupling (PCC). It also includes a variable-speed wind turbine modeled as a PQ source and connected via a step-up transformer, a three-phase load, and a battery energy storage system (BESS) interfaced through a voltage-source inverter. The system parameter data has been referenced as in [25]. The BESS employs two advanced control strategies to enhance system stability. The first is an enhanced power control

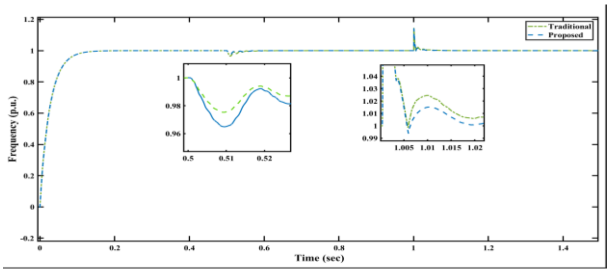

Fig.5 Response of controller for the proposed method (under three-phase fault) on frequency at the PCC

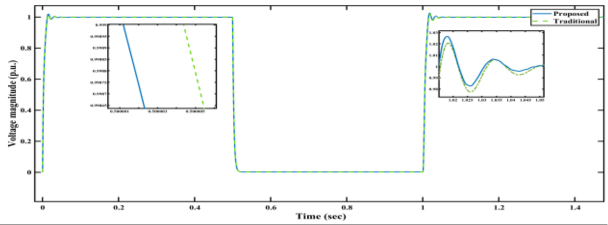

Fig.6 Response of controller for the proposed method (under three-phase fault) on voltage magnitude at the PCC.

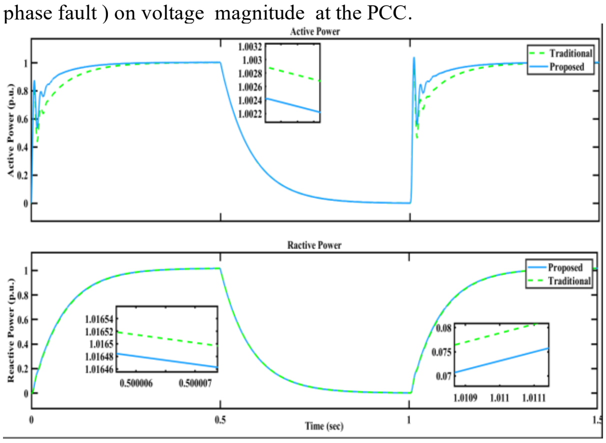

Fig.7 Response of controller for the proposed method (under three-phase fault) on active and reactive power at the PCC.

scheme for voltage support, which dynamically injects or absorbs reactive power to regulate the voltage at Bus 3. The second is a virtual inertia emulation mechanism that modulates active power to mimic synchronous generator behaviour, thereby reducing the rate of change of frequency ((df/dt)) and mitigating frequency deviations. Simulation scenarios typically include wind units' switching, load switching, and three-phase faults to evaluate how the BESS simultaneously stabilizes voltage and frequency.

3.2 Studied scenarios

The performance of the proposed control strategy is evaluated under two distinct scenarios to assess its effectiveness in improving system dynamics under multiple disturbances, particularly in weak grid conditions. These scenarios are described as follows:

- Case 1: Three-phase fault conditions
- Case 2: Load switching

4. Results and discussion

In this section, the MATLAB/Simulink R2024b is employed to achieve the simulation results that are showcased. Personal computer including an AMD Ryzen 7 with 3.30 GHz CPU, 16 GB RAM, and 1TB internal hard drive are used to run the simulation outcomes. The proposed control scheme demonstrates superior dynamic response, improved damping characteristics compared with existing work [7], which makes it highly suitable for modern power systems with high renewable penetration and weak grid conditions.

4.1 Dynamic response against three-phase fault conditions

The dynamic response of weak grid due to grid faults is more complex and a critical aspect. Therefore, this research work makes intensive analysis of dynamic performance of the proposed scheme and its influences on frequency and voltage dynamics. The first study case is a three-phase-to-ground fault that occurs at the PCC during dynamic events around 0.5 s (three fault occurrence) and 1.0 s (fault clearance). Two schemes, proposed and traditional schemes, are implemented and compared to validate the impact of the proposed control scheme in enhancing the dynamics. For frequency response as shown in Fig. 5, when the fault initiated at 0.5 s, the proposed method shows a smaller undershoot and faster recovery compared to the traditional one. After fault clearance, the proposed method has lower peak deviation as illustrated in Fig.5.
Meanwhile, the voltage dynamic response of the proposed method is tested alongside the traditional decoupling method. During recovery after faults clearance, proposed method shows faster voltage restoration and Less oscillation (better damping) as depicted in Fig.6.
Both active and reactive powers are affected by the dynamics of frequency and voltages as shown in Fig 7. Controller overshot after the recovery may be higher than the traditional (1.02 pu), but it's still at an acceptable range (1.027 pu). Alternatively, the frequency response of the proposed controller (1.02 pu) is lower than that of the other controller (1.03 pu).

4.2 Load switching

The dynamic performance of the proposed control method compared to the traditional scheme during a sudden heavy load conditions is investigated, focusing on frequency, voltage magnitude, and active/reactive power responses.
A sudden load increase by 50 MW and 2 MVar at 0.5 sec and for 0.5 sec returning to its normal value. In Fig. 8, both methods initially stabilize the frequency at nominal value;

however, during the disturbance, the proposed method demonstrates a smaller frequency deviation and faster recovery, as clearly shown in the zoomed region. In Fig. 9, the voltage profile indicates that the proposed controller achieves quicker restoration following the voltage dip, with reduced oscillations and improved damping compared to the traditional approach. Additionally, while the voltage dropped significantly, the proposed controller only to (0.76 pu), much higher than the traditional controller (0.67 pu). Furthermore, active and reactive power performance are investigated in both controllers as shown in Fig. 10. The active power response shows reduced fluctuations and faster convergence to steady state, while the reactive power response demonstrates more effective voltage support through improved reactive power injection during disturbances.

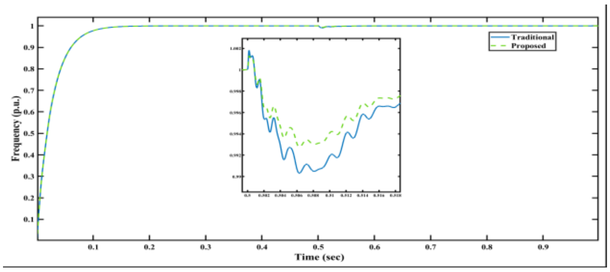

Fig.8 Response of controller for the proposed method (under heavy load condition) on frequency at the PCC

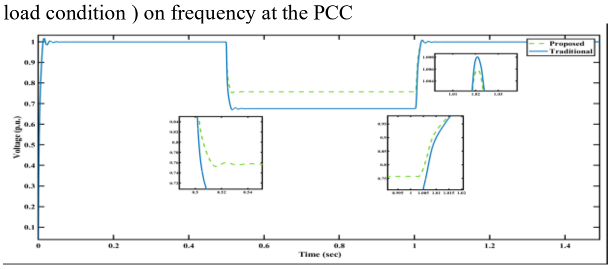

Fig.9 Response of controller for the proposed method (under heavy load condition) on voltage magnitude at the PCC.

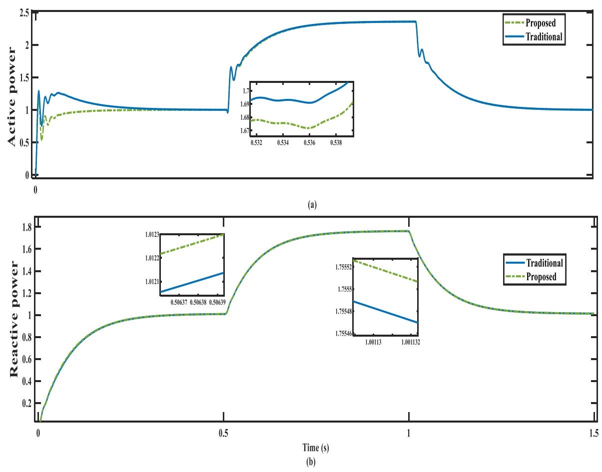

Fig.10 Response of the proposed method (under heavy load condition) on active and reactive power at the PCC.

5. Conclusion

In this paper, a novel control strategy is proposed that utilizes voltage and frequency characteristics in conjunction with active and reactive power channels to enhance the performance of virtual emulation in weak grids. Specifically, a combined control approach based on the rate of change of voltage (dV/dt) and frequency deviation (Δf) is integrated with the active power control loop, while the rate of change of frequency (df/dt) and voltage deviation (ΔV) are incorporated into the reactive power control loop. This coordinated design enables inverter-interfaced energy storage systems, such as battery units, to provide improved dynamic support in weak grid conditions. Moreover, the GVM-DPC is adopted as the inner control loop to accurately track the instantaneous power references, thereby improving the dynamic response of the output power. To validate the effectiveness of the proposed control scheme, two case studies are considered: a three-phase fault disturbance and a sudden heavy load change. The proposed control scheme has been compared with the conventional control technique to show the ability to provide a dynamic support in weak grid conditions.

References

[1] A. Mehrzad *et al.*, "Inertia in renewable power systems: a review of estimation methods and practical implementation," Jan. 01, 2026, *Elsevier Ltd*. doi: 10.1016/j.rser.2025.116246.

[2] M. I. Zaki, R. A. El-Sehiemy, and G. M. Amer, "Efficient fault identification scheme of compensated transmission grid based on correlated reactive power measurements and discrete wavelet transform," *Journal of Electrical Engineering*, vol. 72, no. 4, pp. 217–228, Aug. 2021, doi: 10.2478/jee-2021-0031.

[3] "Investigation on grid-scale BESS providing inertial response support," 2016. [Online]. Available: https://dspace.lboro.ac.uk/2134/23096

[4] "Voltage and frequency regulation to support synchronous generators operation by grid feeding distributed energy resources," 2016.

[5] A. Q. Almousawi and A. Aldair, "Control Strategies for Grid-Tied Inverters Based on Photovoltaic Solar Systems," *IOP Conf. Ser. Mater. Sci. Eng.*, vol. 1067, no. 1, p. 012125, Feb. 2021, doi: 10.1088/1757-899x/1067/1/012125.

[6] Y. Shan, J. Hu, M. Liu, J. Zhu, and J. M. Guerrero, "Model Predictive Voltage and Power Control of Islanded PV-Battery Microgrids with Washout-Filter-Based Power Sharing Strategy," *IEEE Trans. Power Electron.*, vol. 35, no. 2, pp. 1227–1238, Feb. 2020, doi: 10.1109/TPEL.2019.2930182.

[7] "Fast Coordinated Power Control for Improving Inertial and Voltage Support Capability of Battery Energy Storage Systems," *CSEE Journal of Power and Energy Systems*, 2025, doi: 10.17775/cseejpes.2022.06140.

[8] E. Banguero, A. Correcher, Á. Pérez-Navarro, F. Morant, and A. Aristizabal, "A review on battery charging and discharging control strategies: Application to renewable energy systems," Apr. 01, 2018, *MDPI AG*. doi: 10.3390/en11041021.

[9] J. Su, K. Li, Y. Li, C. Xing, and J. Yu, "A Novel State-of-Charge-Based Droop Control for Battery Energy Storage Systems to Support Coordinated Operation of DC Microgrids," *IEEE J. Emerg. Sel.*

Top. Power Electron., vol. 11, no. 1, pp. 312–324, Feb. 2023, doi: 10.1109/JESTPE.2022.3149398.

[10] Y. Huang, X. Yuan, J. Hu, P. Zhou, and D. Wang, “DC-Bus Voltage Control Stability Affected by AC-Bus Voltage Control in VSCs Connected to Weak AC Grids,” *IEEE J. Emerg. Sel. Top. Power Electron.*, vol. 4, no. 2, pp. 445–457, Jun. 2016, doi: 10.1109/JESTPE.2015.2480859.

[11] S. Gao, H. Zhao, Y. Gui, D. Zhou, and F. Blaabjerg, “An improved direct power control for doubly fed induction generator,” *IEEE Trans. Power Electron.*, vol. 36, no. 4, pp. 4672–4685, Apr. 2021, doi: 10.1109/TPEL.2020.3024620.

[12] A. M. Dahman, R. A. El Sehiemy, M. I. Zaki, and A. A. A. El-Ela, “Ground/Phase Detection of Power Transformers’ Faults with Matrix-Based Fault Representation,” in *2021 22nd International Middle East Power Systems Conference (MEPCON)*, IEEE, Dec. 2021, pp. 144–149. doi: 10.1109/MEPCON50283.2021.9686259.

[13] P. Cheng, C. Wu, F. Ning, and J. He, “Voltage modulated dpc strategy of dfig using extended power theory under unbalanced grid voltage conditions,” *Energies (Basel).*, vol. 13, no. 22, Nov. 2020, doi: 10.3390/en13226077.

[14] H. Chojaa *et al.*, “Enhancement of Direct Power Control by Using Artificial Neural Network for a Doubly Fed Induction Generator-Based WECS: An Experimental Validation,” *Electronics (Switzerland)*, vol. 11, no. 24, Dec. 2022, doi: 10.3390/electronics11244106.

[15] Y. A. Alturki, A. A. Alhussainy, S. M. Alghamdi, and M. Rawa, “A Novel Point of Common Coupling Direct Power Control Method for Grid Integration of Renewable Energy Sources: Performance Evaluation among Power Quality Phenomena,” *Energies (Basel).*, vol. 17, no. 20, Oct. 2024, doi: 10.3390/en17205111.

[16] Y. Gui, X. Wang, F. Blaabjerg, and D. Pan, “Control of Grid-Connected Voltage-Source Converters: The Relationship between Direct-Power Control and Vector-Current Control,” Jun. 01, 2019, *Institute of Electrical and Electronics Engineers Inc.* doi: 10.1109/MIE.2019.2898012.

[17] M. Karimi-Ghartemani, H. Karimi, and M. R. Iravani, “A magnitude/phase-locked loop system based on estimation of frequency and in-phase/quadrature-phase amplitudes,” Apr. 2004. doi: 10.1109/TIE.2004.825282.

[18] J. Ma, Y. Yang, X. Che, G. Liu, Y. Guo, and W. Xu, “Magnitude and Phase Compensation in the Phase-Locked Loop of a Permanent Magnet Synchronous Motor-Driven Single-Rotor Air-Conditioning Compressor,” *IEEE Access*, 2026, doi: 10.1109/ACCESS.2026.3667589.

[19] M. I. Zaki, T. F. Megahed, and S. M. Abdelkader, “Efficient Smart Grid Fault-Identification Approach with Photovoltaic- Distributed Generators Based on Monitoring of Current / Voltage Signals,” *Renewable Energy and Power Quality Journal*, no. 20, pp. 161–166, 2022, doi: 10.24084/repqj20.252.

[20] L. Shang, X. Dong, C. Liu, and Z. Gong, “Fast Grid Frequency and Voltage Control of Battery Energy Storage System Based on the Amplitude-Phase-Locked-Loop,” *IEEE Trans. Smart Grid*, vol. 13, no. 2, pp. 941–953, Mar. 2022, doi: 10.1109/TSG.2021.3133580.

[21] U. Datta, A. Kalam, and J. Shi, “Battery energy storage system for aggregated inertia-droop control and a novel frequency dependent state-of-charge recovery,” *Energies (Basel).*, vol. 13, no. 8, Apr. 2020, doi: 10.3390/en13082003.

[22] S. Zhang, W. Qiao, and L. Qu, “A Decoupled Droop Control Strategy for Cascaded Multicell Inverter with Low-Frequency Modulation.”

[23] “Fast Coordinated Power Control for Improving Inertial and Voltage Support Capability of Battery Energy Storage Systems,” *CSEE Journal of Power and Energy Systems*, 2025, doi: 10.17775/cseejpes.2022.06140.

[24] A. Abdul and R. Altahir, “Park and Clark Transformations Park and Clark Transformations: A Short Review.” [Online]. Available: https://www.microsemi.com/document-portal/doc_view/132799-park-inverse-park-and-clarke-

[25] T. Zhao, A. Parisio, and J. V. Milanovic, “Distributed Control of Battery Energy Storage Systems for Improved Frequency Regulation,” *IEEE Transactions on Power Systems*, vol. 35, no. 5, pp. 3729–3738, Sep. 2020, doi: 10.1109/TPWRS.2020.2974026.